

Effect of aeration rate on membrane fouling alleviation in conventional and internal circulation membrane-coupled moving bed biofilm reactors

Ping Yang, Li-ping Wei, Hui-qiang Li*

College of Architecture and Environment, Sichuan University, Chengdu 610065, China, Tel.: +8618980668020; email: lhq_scu@163.com (H.-q. Li), Tel.: +8618602804508; email: yping63@163.com (P. Yang), Tel.: +8613197233099; email: 2941568634@qq.com (L.-p. Wei)

Received 14 May 2023; Accepted 21 August 2023

ABSTRACT

A conventional membrane-coupled moving bed biofilm reactor (Mc-MBBR, R1) and an internal circulation Mc-MBBR (ICMc-MBBR, R2) were operated in parallel to investigate the effects of aeration rate on membrane fouling mitigation. With the aeration rates of 0.1, 0.2 and 0.4 m³/h, the concentration of mixed liquor suspended solids (MLSS) was 1,343 ± 112, 2,566 ± 150 and 2,156 ± 134 mg/L in R1, and the value was 1,523 ± 108, 3,426 ± 196 and 2,246 ± 151 mg/L in R2, respectively. Aeration in the membrane unit and internal circulation in MBBR unit not only increased scour and collision, but also changed the particle-size distribution, extracellular polymeric substances, molecular weight distribution and MLSS concentration. Generation of membrane fouling included two periods: smooth-increase stage and abrupt-increase stage. Particle size below 10 μm and molecular weight above 100 kDa played important roles in smooth-increase stage. Increase of aeration rate and decrease of MLSS concentration delayed the initial formation of cake layer, and the appearance of abrupt-increase stage would be postponed. In the abrupt-increase stage, the value of protein/polysaccharide showed negative correlation with dTMP_r/dt and MLSS concentration showed positive correlation with dTMP_r/dt. Finally, aeration in the membrane unit and the configuration of the internal circulation MBBR mitigated the membrane fouling effectively.

Keywords: Membrane-coupled moving bed biofilm reactor; Membrane fouling; Aeration rate; Internal circulation; Comprehensive analysis

1. Introduction

Moving bed biofilm reactor (MBBR), with the advantages of high treatment capacity and high biomass concentration, dispensable backwashing and little sludge production, has been widely used to treat different kinds of wastewater [1]. However, poor fluidization state of bio-carriers is a common problem in MBBR process, and to add baffles is a usual method to enhance the fluidization state and to accelerate mass transfer rate in practical applications. In addition, it has been proved that the sludge in MBBR is difficult to settle [2]. Membrane separation technology can be used to overcome the disadvantage of MBBR because of the good performance on solid–liquid separation [3]. Membrane-coupled

moving bed biofilm reactor (Mc-MBBR) has been reported to enhance organic pollutants and nutrients removal efficiencies by maintaining multifunctional microbes [4].

Membrane fouling is the stumbling block on the widespread applications of membrane filtration [5]. membrane fouling is a result of interaction between the suspension and membrane surface. Mixed liquor properties, operating conditions and organic components, such as extracellular polymeric substances (EPS) and soluble microbial products (SMP), have been reported to possess complex relationships with membrane fouling [6–8]. In recent years, there were some reports on membrane fouling in the Mc-MBBR. Jamal Khan et al. [9] claimed that the Mc-MBBR mitigated membrane fouling effectively when compared with conventional membrane bioreactor and the opinion has been confirmed

* Corresponding author.

by other researchers [2,10]. Besides, aeration was a common way to mitigate membrane fouling in membrane filtration process. Rahimi et al. [11] studied the effect of aeration on membrane fouling in Mc-MBBR, however, only the relationship between EPS and membrane fouling was analyzed. Zhang et al. [12] discovered that high aeration rate led to more protein and polysaccharide in the supernatant, more loose bound extracellular polymeric substances, less tight bound extracellular polymeric substances, decrease of molecular weight and a lower membrane fouling rate. However, researches were incomplete in terms of membrane fouling and the membrane fouling was complicated during aeration.

The circumstance in MBBR unit of the Mc-MBBR also played an important role in membrane fouling. Deng et al. [13] found that sponge modified bio-carriers could alleviate membrane fouling effectively by lowering the creation of SMP and EPS compared with plastic carriers. However, there was little studies about the effects of internal circulation on membrane fouling. To enhance the fluidization state in a conventional MBBR, an internal circulation MBBR is used usually by adding baffles in the reactors. The baffles inside the MBBR have obvious influences on two phase hydrodynamics and mass transfer in the reactor. The changes of two-phase hydrodynamics have impacts on the dissolved oxygen (DO) distribution, sludge properties and effluent water quality [11]. So, the membrane fouling characteristics of the internal circulation Mc-MBBR would be different from a conventional Mc-MBBR.

Thus, two Mc-MBBRs were operated in parallel in this study. The main objects of this study were to investigate the effects of aeration on alleviating membrane fouling in a conventional Mc-MBBR and an internal circulation Mc-MBBR (ICMc-MBBR) by comprehensive analysis. The variations of transmembrane pressure (TMP), membrane resistance, EPS, particle-size distribution (PSD) and molecular weight distribution (MWD) were monitored to analyze the characteristics of membrane fouling under different aeration rates.

2. Materials and methods

2.1. Set-up and operation of the Mc-MBBRs

Two lab-scale Mc-MBBRs were set-up in this study. R1 was an internal circulation Mc-MBBR with two baffles in MBBR unit and R2 was a conventional Mc-MBBR. Both of the MBBR units were 30 cm × 10 cm × 30 cm with the effective volume of 8.1 L. The dimension of membrane filtration units was 10 cm × 10 cm × 30 cm. The dimension of bio-carrier was Φ10 × 10 mm, with density of 0.96–0.98 g/cm³ and specific surface area of around 1,200 m²/m³. The filling ratio of bio-carriers was around 30% in the MBBR units, and the bio-carriers were fluidized with an aeration rate of 0.2 m³/h throughout the experiment. In membrane filtration unit, a PVDF hollow membrane module with mean pore size of 0.2 μm was set vertically in the middle of the MBR unit.

Seed sludge of the two reactors was obtained a municipal wastewater treatment plant in Chengdu, China. The sludge was acclimated for a week with the synthetic wastewater below before inoculation. Initial sludge concentration in the two reactors was around 1,000 mg/L. The two reactors were operated by intermittent feeding for 5 d after the inoculation. During this period, the synthetic wastewater

was fed every 12 h. Then, continuous influent was adopted with sludge reflux for one week. After that, sludge reflux was stopped and the reactors were continuously operated for another two months before the experiments.

Hydraulic retention time (HRT) of the two MBBR units was maintained around 14 h during the experiments. Temperature of the whole Mc-MBBR was controlled at 25°C ± 2°C. Taking the energy consumption into account, different aeration rates (0.1, 0.2 and 0.4 m³/h) were adopted in the membrane filtration units. The permeate flux of the membrane was 5.35 × 10⁻⁷ m³/(m²·s) and no sludge was discharged during the experiments. The effluent wastewater quality of the two MBBRs was relative stable before this study. The suction of the membrane was terminated when the TMP exceeded 40 kPa in one membrane module. After that, the two membrane modules were taken out of the units and cleaned by deionized water and soaked with NaClO solution for subsequent experiments.

2.2. Synthetic wastewater

Synthetic wastewater was used for the two reactors to ensure a relative stable influent wastewater quality, so as to study the effect of aeration rate on membrane fouling alleviation in the two reactors. The synthetic wastewater was prepared with tap water, including glucose of 1,000 mg/L, NH₄Cl of 76 mg/L, NaHCO₃ of 476 mg/L, KH₂PO₄ of 22 mg/L and trace elements. The trace elements were consistent with those used by Gu et al. [14].

2.3. Analytical methods

2.3.1. Membrane foulants analysis

The measure of membrane foulants was conducted as following. The cake layers on membrane surface were removed by a sponge and resuspended with 3 L of deionized water. The mixed liquor suspended solids (MLSS), mixed liquored volatile suspended solids (MLVSS) and EPS of the resuspended foulants were analyzed as methods mentioned in 2.3.3 and 2.3.5. The membrane permeability after removing the cake layer was evaluated by recording the TMP with the filtration of deionized water. Then the membrane modules were soaked with 0.5% NaClO solution for one week. After that, the membrane permeability was evaluated by the filtration of deionized water once more.

2.3.2. Membrane resistance analysis

Total membrane resistance (R_t) can be divided into three parts, including cake layer resistance (R_c), gel layer resistance (R_g) and intrinsic membrane resistance (R_m). The membrane resistance of each part was described by Wei et al. [15]. The calculation of membrane resistance could be expressed as follows:

$$J = \frac{\Delta P}{\mu R_t} = \frac{\Delta P}{\mu (R_m + R_c + R_g)} \quad (1)$$

$$R_c = R_t - (R_m + R_g) = R_t - \frac{\Delta P_1}{\mu_0 \times J_1} \quad (2)$$

$$R_m = \frac{\Delta P_0}{\mu_0 \times J_0} \quad (3)$$

where ΔP is the TMP (Pa); ΔP_0 is the initial TMP; ΔP_1 is the TMP after mechanical cleaning; μ is the dynamic viscosity (Pa·s); μ_0 is the dynamic viscosity of clean water (Pa·s); J is the membrane flux ($\text{m}^3/\text{m}^2\cdot\text{s}$); J_0 is the initial membrane flux ($\text{m}^3/\text{m}^2\cdot\text{s}$); J_1 is the membrane flux after mechanical cleaning ($\text{m}^3/\text{m}^2\cdot\text{s}$); R_t is the total membrane resistance (m^{-1}); R_m is the intrinsic membrane resistance (m^{-1}); and R_s is the gel layer resistance (m^{-1}).

2.3.3. EPS analysis

The extraction of EPS was done based on the heat extraction methods [16]. 60 mL suspension was divided into two samples evenly to analyze different types of EPS. One sample was centrifuged at a rotation rate of $4,000 \times g$ for 10 min, then being filtrated through a $0.45 \mu\text{m}$ filter paper. The filtrate was regarded as soluble extracellular polymeric substances (S-EPS). The other sample was heated at 80°C for 10 min at first, and the suspension was then centrifuged at $4,000 \times g$ for 10 min. After being filtrated through a $0.45 \mu\text{m}$ filter paper, the filtrate was regarded as total extracellular polymeric substances (T-EPS). The difference between T-EPS and S-EPS was regarded as bound extracellular polymeric substances (B-EPS). Protein (PN) and polysaccharide (PS) were determined according to Gu et al. [14].

2.3.4. Molecular weight distribution analysis

The filtrate obtained from centrifuged suspension sample without heating was characterized by the MWD analysis. The MWD was determined with membrane filtration method according to Gao et al. [17], and computed based on permanganate value.

2.3.5. Other items

MLSS and MLVSS were analyzed according to standard methods [18]. The PSD was measured using the Mastersizer Z2000 (Malvern, UK). DO and temperature were monitored by a portable meter (YSI550A, YSI, USA), and pH was monitored by a pH meter (PHS-25, Leici, China).

3. Results

3.1. Basic parameter of the Mc-MBBRs

The parameters of MBBR units are shown in Table 1. Average MLSS concentration in R2 was 233 mg/L higher

Table 1

Average values of EPS, mean particle size (PS), molecular weight distribution, and MLSS concentration in two MBBR units, along with the standard deviation

	EPS (mg/g·MLSS)		MWD (mg/g·MLSS)				Mean PS (μm)	MLSS (mg/L)
	S-EPS	B-EPS	>100 kDa	50–100 kDa	10–50 kDa	<10 kDa		
R1	16.2 ± 1.1	19.4 ± 1.3	23.3 ± 2.3	20.5 ± 3.2	32.0 ± 1.2	27.9 ± 3.6	383	$1,321 \pm 136$
R2	13.5 ± 1.0	33.0 ± 2.1	19.4 ± 0.9	19.3 ± 3.0	32.2 ± 5.9	29.0 ± 2.2	409	$1,554 \pm 224$

than that in R1. The value of MLVSS/MLSS was 0.77 in both reactors. Besides, the concentration of MW above 100 kDa in R1 was 3.95 mg/L higher than that in R2. The S-EPS and B-EPS in R1 were 16.3 and 19.4 mg/g·MLSS, respectively, and they were 13.5 and 33 mg/g·MLSS in R2. The value of protein/polysaccharides (PN/PS) was 2.2 in R1, more than 2 times higher than that in R2 in the mixed liquid. As for the membrane filtration units, the aeration rate was controlled at 0.1, 0.2 and $0.4 \text{ m}^3/\text{h}$, respectively. The concentration of MLSS was $1,343 \pm 112$, $2,566 \pm 150$ and $2,156 \pm 134 \text{ mg/L}$ in R1, for each aeration level. And the value was $1,523 \pm 108$, $3,426 \pm 196$ and $2,246 \pm 151 \text{ mg/L}$ in R2, respectively.

3.2. Evolution of transmembrane pressure

Fig. 1 illustrates the evolution of TMP at different aeration rates in two Mc-MBBRs. The variation of TMP in two reactors followed similar trend, which increased slowly at first, and followed by an abrupt-increase stage. Great differences existed in the fouling rate and the appearance of abrupt-increase stage. The fouling rate in smooth-increase stage ($d\text{TMPs}/dt$) was 0.098, 0.294 and 0.172 kPa/d in R1 and 0.004, 0.115 and 0.083 kPa/d in R2 when the aeration rate was 0.1, 0.2 and $0.4 \text{ m}^3/\text{h}$, respectively. The fouling rate in abrupt-increase stage ($d\text{TMPPr}/dt$) was 6.01, 9.70 and 7.81 kPa/d in R1 and 11.14, 12.83 and 9.6 kPa/d in R2 when the aeration rate was 0.1, 0.2 and $0.4 \text{ m}^3/\text{h}$, respectively. Comparing the two reactors under the same aeration rate,

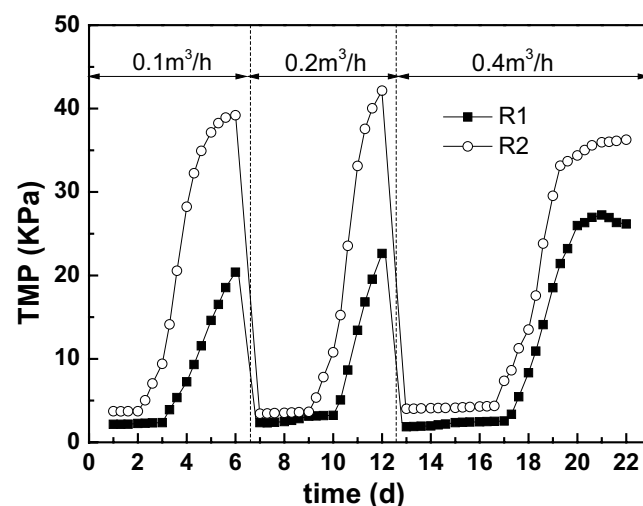


Fig. 1. Evolution of transmembrane pressure under different aeration rates.

the dTMPs/dt of R1 was at least 23% higher than that of R2, while when it came to dTMPr/dt, the result was converse. The abrupt-increase stage of R2 appeared earlier than that of R1, and the final TMP value of R2 was higher than R1. Additionally, with the increase of aeration rate, operation time of both reactors extended from 5 to 9 d and the appearance of abrupt-increase stage was delayed.

Different types of membrane resistance are shown in Table 2. R_m only accounted for less than 6% of R_t , and growing trends of R_m were observed in both reactors. R_c occupied more than 90% of R_t under different aeration rates while R_s accounted less than 4%. The results indicated that cake layer was the main factor inducing membrane fouling. R_t decreased as the aeration rate increased, and R_t of R2 was at least 10% higher than that of R1 at the same aeration rate. Therefore, high aeration rate and internal circulation Mc-MBBR had good effects on membrane fouling mitigation.

3.3. Particle-size distribution

The PSD in the membrane filtration unit under different aeration rates is shown in Fig. 2. Comparing the PSD in two membrane filtration units under the same aeration rate, the mean particle size of R1 was smaller than that in R2. The mean particle size was 272, 208 and 332 μm in R1 and was 318, 367 and 437 μm in R2 when the aeration rate was 0.1, 0.2 and 0.4 m^3/h , respectively. The mean particle size showed an increasing trend as the aeration rate increased from 0.1 to 0.4 m^3/h in membrane filtration unit of R2.

The membrane filtration unit of R1 tended to contain more tiny flocs (below 10 μm) than in R2 at the same aeration rate. Interestingly, the particle size below 10 μm accounted for 6.75% and 2.34% in membrane filtration units of R1 and R2 when the aeration rate was 0.2 m^3/h , while only accounted for 4% and 0.95% when the aeration rate was 0.4 m^3/h .

3.4. Extracellular polymeric substances

The changes of EPS in membrane filtration units are shown in Fig. 3a. The T-EPS in the membrane filtration unit of R2 was 25, 20 and 26 $\text{mg}/\text{g}\text{-MLSS}$ when the aeration rate was 0.1, 0.2 and 0.4 m^3/h , which was 57, 43 and 46 $\text{mg}/\text{g}\text{-MLSS}$ in R1, respectively. R1 encompassed more EPS, whether S-EPS or B-EPS, than R2 during the whole period. The value of PN/PS was 1.37, 0.43 and 0.63 in R1 when the aeration rate was 0.1, 0.2 and 0.4 m^3/h , which was 0.78, 0.59 and 0.53 in R2, respectively.

Cake layer made an important contribution to the membrane resistance. The EPS of sludge on the membrane surface is shown in Fig. 3b. The T-EPS on the membrane surface in R1 was 47, 59 and 46 $\text{mg}/\text{g}\text{-MLSS}$ when the aeration rate was 0.1, 0.2 and 0.4 m^3/h , which was 64, 75 and 56 $\text{mg}/\text{g}\text{-MLSS}$ in R2, respectively. R2 contained more PS and PN than R1 during the whole period. Comparing the concentration of EPS under different aeration rates, the EPS concentration (especially polysaccharides) was the largest when the aeration rate was 0.2 m^3/h . The value of PN/PS in R1 was 1.87, 0.61 and 1.16, while was 1.82, 0.47 and 0.91 in R2 when the

Table 2
Variation of membrane resistance types under different aeration rates

	Aeration rate m^3/h	R_t		R_m			R_c		R_s	
		10^{11} m^{-1}	10^{11} m^{-1}	%	10^{11} m^{-1}	%	10^{11} m^{-1}	%		
R1	0.1	1,058.43	14.68	1.39	1,042.94	97.57	0.82	0.08		
	0.2	507.87	17.00	3.35	475.31	93.59	15.56	3.06		
	0.4	417.11	24.95	5.98	388.77	95.56	3.39	0.83		
R2	0.1	1,140.97	44.38	3.89	1,095.78	95.68	0.81	0.07		
	0.2	967.13	48.67	5.03	910.59	94.57	7.87	0.82		
	0.4	778.58	52.54	6.75	723.2	92.89	2.84	0.36		

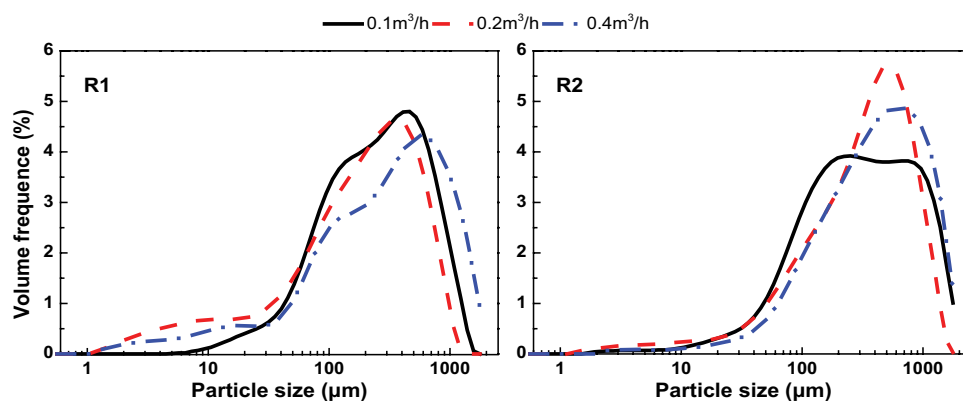


Fig. 2. Particle-size distribution in membrane filtration units under different aeration rates.

eration rate were 0.1, 0.2 and 0.4 m³/h, respectively. The difference of PN/PS between the sludge in membrane filtration unit and the membrane surface was attributed to the degradation and secretion of EPS. Previous studies found that the cake layer showed higher biodegradation ability than those in the mixed liquor, and PN had much higher biodegradation rates than PS [19].

3.5. Molecular weight distribution

The MWD of the S-EPS before and after membrane filtration under different aeration rates is shown in Fig. 4. The molecular weight below 100 kDa was similar before and after membrane with aeration rate of 0.1 and 0.2 m³/h, the opposite phenomenon occurred in aeration rate of 0.4 m³/h was attributed to the acidification of the effluent. The molecular weight above 100 kDa decreased obviously after filtration. In R2, the molecular weight above 100 kDa before membrane was 24.2, 38.7 and 22.4 mg/L, while it was 9.1, 31 and 14 mg/L after filtration when the aeration rate was 0.1, 0.2 and 0.4 m³/h, respectively. The MWD performed the similar variation pattern before and after filtration in R1. The results indicated that the membrane could retain part of the soluble organic compounds, and the retention effect was the worst at the aeration rate of 0.2 m³/h. Under different aeration rates, the value of molecular weight above 100 kDa was the highest when the aeration rate was 0.2 m³/h. As for

the MWD under the same aeration rate, R1 tended to keep more fraction of molecular weight above 100 kDa than R2.

4. Discussion

4.1. Possible key factors affecting membrane fouling

Particle size and EPS like substrates exert important roles in membrane fouling. A previous study made by Shen et al. [20] indicated that small flocs would increase hydraulic cake resistance and osmotic pressure-induced resistance of the membrane module. Previous study found that smaller particles could retain higher levels of bound EPS compared with large flocs, and it was easier to form a gel layer when there were a larger proportion of soluble organic substances and a smaller particle size [21]. Thus, it was hard for large flocs to attach the membrane surface because of the shear force caused by aeration in the beginning of fouling formation. During the experiments, with the aeration rate of 0.2 m³/h, the particle size below 10 μm accounted for 6.75% and 2.34% in membrane filtration units of R1 and R2, with corresponding dTMPs/dt values of 0.294 and 0.115 kPa/d. When the aeration rate increased to 0.4 m³/h, the particle size below 10 μm accounted for 4% and 0.95% for R1 and R2, and the dTMPs/dt value was 0.172 kPa/d and 0.083 kPa/d, respectively. The value of dTMPs/dt showed a significant correlation with particles below 10 μm (the correlation

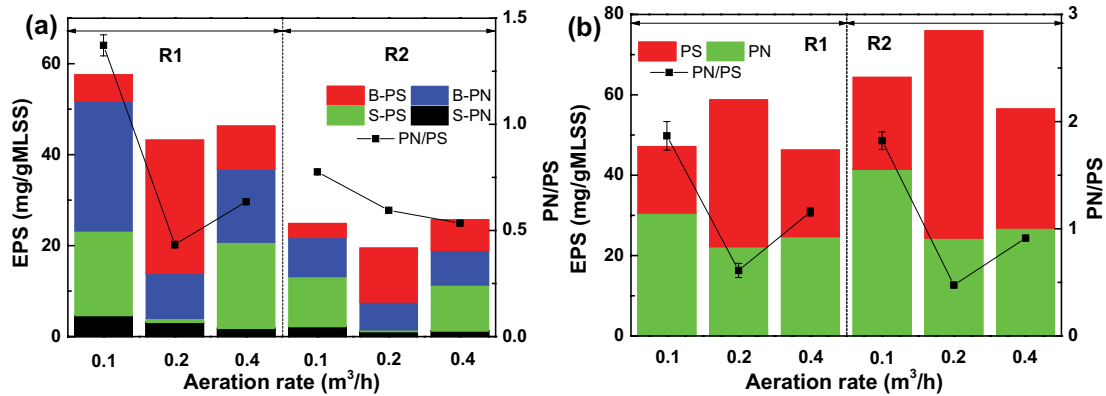


Fig. 3. Variations of EPS under different aeration rates (a) the EPS of membrane filtration units and (b) the EPS of membrane surface.

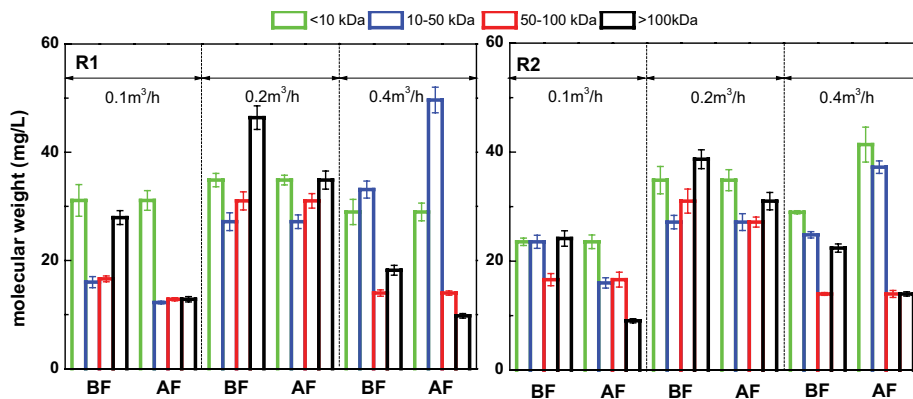


Fig. 4. Molecular weight distribution of S-EPS under different aeration rates (BF: before filtration; AF: after filtration).

coefficient ($r_p = 0.92$). The result indicated that small particles played an important role in the smooth-increased stage of TMP, and it could be one of the reasons for the highest R_g ($15.56 \times 10^{11} \text{ m}^{-1}$ for R1 and $7.87 \times 10^{11} \text{ m}^{-1}$ for R2) when the aeration rate was $0.2 \text{ m}^3/\text{h}$. In addition, r_p between the molecular weight above 100 kDa and $d\text{TMP}_p/dt$ was 0.61. The result was consistent with the research by Zhou et al. [22], who found that the SMP related compounds played an important role in the smooth-increased stage of membrane fouling, especially the compounds with high MWD.

It could be noticed that there was a sudden change after the smooth-increased stage under all conditions, which was associated with the initial formation of cake layer. The formation of cake layer could be analyzed from hydrodynamic and thermodynamic properties. The hydrodynamic property was associated with the flocs approached to the surface of membrane, while thermodynamic property was responsible for the attachment of the flocs on membrane surface [7]. The increase of aeration rate could enhance shear force obviously, resulting in obstruction for particles, especially large flocs, attaching to the membrane surface. Therefore, the aeration rate played an important role on the initial formation of cake layer, and the appearance of abrupt-increase stage in both reactors was extended from 5 to 9 d when the aeration rate increased from 0.1 to $0.4 \text{ m}^3/\text{h}$. The higher the aeration rate was, the later the abrupt-increased stage appeared. Except for aeration rate, the MLSS concentration was another factor affecting the appearance time of abrupt-increased stage. As mentioned in sections 3.1 and 3.2, it was obvious that the abrupt-increased stage appeared in advance with the increase of MLSS concentration.

Lee and Kim [23] found that membrane fouling was sensitive to MLSS concentration, and similar conclusion was discovered in current research. The correlation analysis showed that the r_p between MLSS concentration in membrane filtration unit and the value of $d\text{TMP}_p/dt$ exhibited a significant correlation ($r_p = 0.68$). In addition, previous study found that the value of PN/PS had effects on the hydrophobicity and electrostatic repulsive force and positively correlated to filtration resistance [16]. The r_p between PN/PS in the membrane filtration unit and $d\text{TMP}_p/dt$ was -0.63 in this study. Moreover, Pourbozorg et al. [24] found that the presence of turbulence moderated the membrane fouling and reduced the corresponding increasing rate of TMP ($d\text{TMP}/dt$). Briefly, the MLSS concentration and the value of PN/PS played important roles in the abrupt-increased stage.

4.2. Alleviation of membrane fouling by aeration and internal circulation

Aeration played an important role in membrane fouling in present study. Previous research had confirmed that the particle size would decrease when the aeration rate increased [25]. In present study, there were more small particles (the particle size below $10 \mu\text{m}$) in membrane filtration units when the aeration rate was $0.2 \text{ m}^3/\text{h}$, comparing with the aeration rates of 0.1 and $0.4 \text{ m}^3/\text{h}$. The phenomenon would be attributed to the mechanism of particle re-aggregation. Many researchers agreed with that the rate of floc formation was a balance between breakage and aggregation with flocs

[26]. The shear force, MLSS, and composition of EPS in the sludge had sever effects on the ability of floc formation [27]. The shear force would increase with the elevation of aeration rate, which was conducive to create smaller particles. However, the EPS also played an important role in flocculation of sludge. The T-EPS concentration in the membrane filtration unit of R1 and R2 was 43 and 20 mg/g-MLSS with the aeration rate of $0.2 \text{ m}^3/\text{h}$, and was 46 and 26 mg/g-MLSS with the aeration rate of $0.4 \text{ m}^3/\text{h}$. Moreover, the mean particle size was $332 \mu\text{m}$ for R1 and $437 \mu\text{m}$ for R2 with the aeration rate of $0.4 \text{ m}^3/\text{h}$, which was larger than the ones ($208 \mu\text{m}$ for R1 and $367 \mu\text{m}$ for R2) with the aeration rate of $0.2 \text{ m}^3/\text{h}$.

Aeration not only affected the PSD, but also influenced the conversion of EPS. EPS could be degraded by various microorganism [7]. It was worth noting that the two membrane filtration units contained minimal amount of EPS when the aeration rate was $0.2 \text{ m}^3/\text{h}$ (as shown in Fig. 3a). The result could be explained by the degradation of EPS. When the aeration rate was $0.1 \text{ m}^3/\text{h}$, the microbial activity was influenced because of the relative low oxygen concentration. The microbial degradation of EPS was improved by increasing the aeration rate to $0.2 \text{ m}^3/\text{h}$. When the aeration rate increased to $0.4 \text{ m}^3/\text{h}$, the microbes were stimulated so as to secrete more EPS comparing with aeration rate of $0.2 \text{ m}^3/\text{h}$ [12]. The explanation was also confirmed by the change of MLSS concentration in the membrane filtration units. As no sludge was recycled to the MBBR units, the membrane filtration unit could be regarded as a sludge thickening tank. In section 3.1, the MLSS concentration in both MBBR units was relative stable throughout the experiments. The MLSS concentration in the membrane filtration units with aeration rate of $0.4 \text{ m}^3/\text{h}$ was $2,156 \pm 134 \text{ mg/L}$ in R1 and $2,246 \pm 151 \text{ mg/L}$ in R2, which was much lower than aeration rate of $0.2 \text{ m}^3/\text{h}$ ($2,566 \pm 150 \text{ mg/L}$ in R1 and $3,426 \pm 196 \text{ mg/L}$ in R2). The results indicated that some sludge was biodegraded.

The effluent of the MBBR unit was also important although it didn't contact with the membrane directly. The baffle inside the MBBR unit was an important geometric parameter and had an obvious influence on two phase hydrodynamics and mass transfer in the reactor. The placement of baffles in the reactor would enhance the liquid velocity in the reactor [28], which increased the frequency and intensity of collision among bio-carriers and flocs, and affected properties of mixed liquor. The mean particle size of R1 was $383 \mu\text{m}$, which was $26 \mu\text{m}$ smaller than that in R2. The increase of collision resulted in more tiny particles, which had an important role on membrane fouling. Besides, The EPS in R1 was 22.7 mg/g-MLSS which was less than in R2, and the S-EPS in R1 was 2.7 mg/g-MLSS which was higher than in R2. Li et al. [29] had found that higher concentration of S-EPS and lower concentration of B-EPS were recorded in higher shear stress. The difference of SMP in R1 and R2 was due to the enhancement of fluidization, which promoted the decomposition and conversion of B-EPS to S-EPS. Besides, the MW distribution of MBBR units in this study also confirmed the results. The MW above 100 kDa in R1 was 23.4 mg/L , which was 4 mg/L higher than that in R2. Moreover, the PN/PS in R1 was 2.17, which was more than 2 times higher than that in R2. Previous analysis had

indicated that high PN/PS was beneficial for the membrane fouling mitigation. Furthermore, the MLSS of MBBR unit in R1 was 233 mg/L which was less than in R2. It was due to the smaller particles in R1, which ran off easier than the larger ones. Therefore, the internal circulation Mc-MBBR mitigated membrane fouling by enhancing the value of PN/PS and lowering the concentration of the MLSS.

5. Conclusion

Effect of different aeration rates on membrane fouling was studied in two membrane-coupled MBBRs, with and without internal circulation in the MBBR unit. According to the variation of TMP, the process of membrane fouling was divided into the smooth-increase stage, which was affected predominantly when the particle size was below 10 μm and the molecular weight was above 100 kDa, and the abrupt-increase stage was mainly originated from the initial formation of cake layer which was affected by the aeration rate and MLSS concentration. Internal circulation structure and suitable aeration rate alleviated membrane fouling obviously. Specially, internal circulation configuration in the MBBR unit mitigated membrane fouling by enhancing the value of PN/PS and lowering the concentration of the MLSS. Aeration retarded membrane fouling by affecting the PSD, MWD, EPS and MLSS concentration, and the corresponding optimal aeration rate was 0.2 m^3/h in this experiments.

Acknowledgement

This research was supported by the International Scientific and Technological Innovation and Cooperation Project of Sichuan (No. 2019YFH0170).

References

- [1] Q. Gu, T. Sun, G. Wu, M. Li, W. Qiu, Influence of carrier filling ratio on the performance of moving bed biofilm reactor in treating coking wastewater, *Bioresour. Technol.*, 166 (2014) 72–78.
- [2] F. Chen, X. Bi, H.Y. Ng, Effects of bio-carriers on membrane fouling mitigation in moving bed membrane bioreactor, *J. Membr. Sci.*, 499 (2016) 34–42.
- [3] H.Y. Ng, T.W. Tan, S.L. Ong, Membrane fouling of submerged membrane bioreactors: impact of mean cell residence time and the contributing factors, *Environ. Sci. Technol.*, 40 (2006) 2706–2713.
- [4] S. Yang, F. Yang, Z. Fu, R. Lei, Comparison between a moving bed membrane bioreactor and a conventional membrane bioreactor on organic carbon and nitrogen removal, *Bioresour. Technol.*, 100 (2009) 2369–2374.
- [5] C. Wang, W.N. Chen, Q.Y. Hu, M. Ji, X. Gao, Dynamic fouling behavior and cake layer structure changes in nonwoven membrane bioreactor for bath wastewater treatment, *Chem. Eng. J.*, 264 (2015) 462–469.
- [6] L. Deng, W. Guo, H.H. Ngo, H. Zhang, J. Wang, J. Li, S. Xia, Y. Wu, Biofouling and control approaches in membrane bioreactors, *Bioresour. Technol.*, 221 (2016) 656–665.
- [7] H. Lin, M. Zhang, F. Wang, F. Meng, B. Liao, H. Hong, J. Chen, W. Gao, A critical review of extracellular polymeric substances in membrane bioreactors: characteristics, roles in membrane fouling and control strategies, *J. Membr. Sci.*, 460 (2014) 110–125.
- [8] W. Yang, W. Syed, H. Zhou, Comparative study on membrane fouling between membrane-coupled moving bed biofilm reactor and conventional membrane bioreactor for municipal wastewater treatment, *Water Sci. Technol.*, 69 (2014) 1021–1027.
- [9] S. Jamal Khan, Zohaib-Ur-Rehman, C. Visvanathan, V. Jegatheesan, Influence of biofilm carriers on membrane fouling propensity in moving bed biofilm membrane bioreactor, *Bioresour. Technol.*, 113 (2012) 161–164.
- [10] L. Duan, W. Jiang, Y. Song, S. Xia, S.W. Hermanowicz, The characteristics of extracellular polymeric substances and soluble microbial products in moving bed biofilm reactor-membrane bioreactor, *Bioresour. Technol.*, 148 (2013) 436–442.
- [11] Y. Rahimi, A. Torabian, N. Mehrdadi, M. Habibi-Rezaie, H. Pezeshk, G.R. Nabi-Bidhendi, Optimizing aeration rates for minimizing membrane fouling and its effect on sludge characteristics in a moving bed membrane bioreactor, *J. Hazard. Mater.*, 186 (2011) 1097–1102.
- [12] H. Zhang, H. Yu, L. Zhang, L. Song, Stratification structure of polysaccharides and proteins in activated sludge with different aeration in membrane bioreactor, *Bioresour. Technol.*, 192 (2015) 361–366.
- [13] L. Deng, W. Guo, H.H. Ngo, X. Zhang, X.C. Wang, Q. Zhang, R. Chen, New functional biocarriers for enhancing the performance of a hybrid moving bed biofilm reactor-membrane bioreactor system, *Bioresour. Technol.*, 208 (2016) 87–93.
- [14] Y. Gu, T. Li, H. Li, Biofilm formation monitored by confocal laser scanning microscopy during startup of MBBR operated under different intermittent aeration modes, *Process Biochem.*, 74 (2018) 132–140.
- [15] D. Wei, Y. Tao, Z. Zhang, L. Liu, X. Zhang, Effect of in-situ ozonation on ceramic UF membrane fouling mitigation in algal-rich water treatment, *J. Membr. Sci.*, 498 (2016) 116–124.
- [16] X. Su, Y. Tian, H. Li, C. Wang, New insights into membrane fouling based on characterization of cake sludge and bulk sludge: an especial attention to sludge aggregation, *Bioresour. Technol.*, 128 (2013) 586–592.
- [17] W. Gao, M. Han, X. Qu, C. Xu, B. Liao, Characteristics of wastewater and mixed liquor and their role in membrane fouling, *Bioresour. Technol.*, 128 (2013) 207–214.
- [18] *Water and Wastewater Monitoring Methods*, 2012, Chinese NEPA, China.
- [19] S.M. Hocaoglu, D. Orhon, Fate of proteins and carbohydrates in membrane bioreactor operated at high sludge age, *J. Environ. Sci. Health. Part A Toxic/Hazard. Subst. Environ. Eng.*, 45 (2010) 1101–1108.
- [20] L. Shen, Q. Lei, J. Chen, H. Hong, Y. He, H. Lin, Membrane fouling in a submerged membrane bioreactor: impacts of floc size, *Chem. Eng. J.*, 269 (2015) 328–334.
- [21] H. Lu, Z. Xue, P. Saikaly, S.P. Nunes, T.R. Bluver, W.T. Liu, Membrane biofouling in a wastewater nitrification reactor: microbial succession from autotrophic colonization to heterotrophic domination, *Water Res.*, 88 (2016) 337–345.
- [22] Z. Zhou, F. Meng, X. He, S.R. Chae, Y. An, X. Jia, Metaproteomic analysis of biocake proteins to understand membrane fouling in a submerged membrane bioreactor, *Environ. Sci. Technol.*, 49 (2015) 1068–1077.
- [23] S. Lee, M.H. Kim, Fouling characteristics in pure oxygen MBR process according to MLSS concentrations and COD loadings, *J. Membr. Sci.*, 428 (2013) 323–330.
- [24] M. Pourbozorg, T. Li, A.W.K. Law, Effect of turbulence on fouling control of submerged hollow fibre membrane filtration, *Water Res.*, 99 (2016) 101–111.
- [25] I. Ivanovic, T. Leiknes, Impact of aeration rates on particle colloidal fraction in the biofilm membrane bioreactor (BF-MBR), *Desalination*, 231 (2008) 182–190.
- [26] P. Jarvis, B. Jefferson, J. Gregory, S.A. Parsons, A review of floc strength and breakage, *Water Res.*, 39 (2005) 3121–3137.
- [27] B.Q. Liao, D.G. Allen, I.G. Droppo, G.G. Leppard, S.N. Liss, Surface properties of sludge and their role in bioflocculation and settleability, *Water Res.*, 35 (2001) 339–350.
- [28] P. Lestinsky, M. Vecer, P. Vayrynen, K. Wichterle, The effect of the draft tube geometry on mixing in a reactor with an internal circulation loop – a CFD simulation, *Chem. Eng. Process.*, 94 (2015) 29–34.
- [29] T. Li, A.W.K. Law, Y.S. Jiang, A.K. Harijanto, A.G. Fane, Fouling control of submerged hollow fibre membrane bioreactor with transverse vibration, *J. Membr. Sci.*, 505 (2016) 216–224.